J. Membrane Biol. 196, 135–146 (2003)
DOI: 10.1007/s00232-003-0633-z

The Journal of
Membrane
Biology

Soft Picture of Lateral Heterogeneity in Biomembranes

J. Štrancar, T. Koklič, Z. Arsov
Laboratory of Biophysics, "Jožef Stefan" Institute, Jamova 39, SI-1000 Ljubljana, Slovenia

Received: 7 May 2003/Revised: 24 September 2003

Abstract. Standard methods of characterization of electron paramagnetic resonance (EPR) spectra of spin-labeled biomembranes limit the resolution of lateral heterogeneity to only two or three domain types. This disables examination of the structure—function relationship in complex membranes, which might be composed of a larger number of different domain types. To enable exploration of this kind, a new approach based on analysis of EPR spectra with multi-run, hybrid evolutionary optimization is proposed here. From the multiple runs a quasi-continuous distribution of membrane spectral parameters (order parameter, proportion of spectral component, polarity correction factor, rotational correlation time and broadening constant) can be constructed and presented by a new presentation technique CODE (colored distribution of EPR spectral parameters). Through this the concept of a "soft" picture of membrane heterogeneity is introduced, in contrast to the standard "discrete" domain picture. The "soft" characterization method, established on synthetic spectra, was used to examine the lateral heterogeneity of liposome membranes as well as of membranes of neutrophils from healthy and asthmatic horses. In liposome membranes the determined number of domain types was the same as already established by standard procedures of EPR spectra line-shape interpretation. In membranes of neutrophils a quasi-continuous distribution of membrane domain properties was detected by the new method.

Key words: Complexity of biological membranes — Membrane lateral lipid domains — Electron paramagnetic resonance (EPR) — Hybrid evolutionary optimization (HEO) — Colored Distribution of EPR spectral parameters (CODE)

Correspondence to: J. Štrancar; email: janez.strancar@ijs.si

Introduction

The lateral membrane heterogeneity has been studied intensively in the past few years by many different experimental techniques, e.g., electron paramagnetic resonance (EPR) spectroscopy with spin labeling (Gaffney & Marsh, 1998; Žuvič-Butorac et al., 1999; Ge et al., 1999; Vishnyakova et al., 2000; Arsov, Schara & Štrancar, 2002; Koklič, Šentjurc & Zeisig, 2002), fluorescence resonance energy transfer (Loura, Fedorov & Prieto, 2001), single particle tracking (Tomishige & Kusumi, 1999), atomic force microscopy (Rinia & de Kruijff, 2001), and Raman scattering microscopy (Percot & Lafleur, 2001). EPR is an important method for lateral heterogeneity characterization because it allows studying intact complex systems of cell suspensions. In addition, the time scale of dynamic events that are observed is appropriate (Marsh & Horváth, 1998).

A lateral lipid domain is a spatially defined membrane region that has one or more measurable properties that distinguish it from neighboring regions of the membrane (Bloom & Thewalt, 1995). The particular domain type in general represents a group of domains with equal motional characteristics. In the EPR picture, distinct domain types are characterized with sets of different spectral parameters where each set defines one spectral component. The parameters describe the rate and anisotropy of motion of the spin labels introduced into the membrane, as well as the polarity of spin label environment in the particular domain type. In general, EPR in combination with different characterization methods cannot determine the size or the size distribution of domains of the same type (but *see* Sankaram, Marsh & Thompson, 1992). The proportion of each domain type does not directly represent the area of this domain type but depends on the partitioning of the spin probe molecules between domains. One should also be aware of the possibility that not all the spectral components originate from membrane

domains. Some of them may be a consequence of spin probes in a solution, micelle aggregates of spin probes, etc.

Lateral domain studies are important for showing the interdependence between the lipid domain structure changes and various physiological conditions or activation of various membrane elements such as membrane-bound proteins (Dibble et al., 1996; Hønger et al., 1996; Sok, Šentjurc & Schara, 1999; Žuvič-Butorac et al., 2001; *see also* reviews by Devaux & Seigneuret, 1985; Tocanne et al., 1994; Edidin, 1997). In this respect it was shown that the EPR spectra of different spin labels in different kinds of cells, liposomes, etc. cannot be described with one spectral component determined by a single group of EPR spectral parameters. Instead, EPR spectra should usually be decomposed into at least two spectral components, each described by a separate group of EPR spectral parameters.

The decomposition to at least two spectral domain types is indubitable in the systems composed of different lipid species (including cholesterol or sphingolipids) and/or membrane proteins. The number of spectral components is limited primarily because the interpretation of the results becomes very complicated and unclear due to the large number of spectral parameters (e.g., a characteristic number of spectral parameters is 5 per spectral component). At the same time, no dramatic improvement in the goodness of fit can be achieved, usually due to the too low signal-to-noise ratio value. Finally, the number of spectral components is limited also by the effectiveness of the optimization procedures by which the spectral parameters' extraction is performed. To summarize, interpretation ability, signal-to-noise ratio, and optimization effectiveness usually limit the number of spectral components.

While the signal-to-noise ratio can be improved by a moderated experimental approach, the optimization effectiveness as well as the interpretation ability can be improved by modifying the spectra characterization procedures. A large effort was made to bring the spectral characterization procedures as close as possible to full automation. Different research groups attempted this problem by applying various optimization methods, e.g., deterministic Simplex downhill and Levenberg-Marquardt, stochastic Monte Carlo, maximum-likelihood common-factor analysis (Kirste, 1992; Moens et al., 1993; Chachaty & Soulie, 1995; Eviatar, van der Heide & Levine, 1995; Budil et al, 1996; Della Lunga, Pogni & Basosi, 1998). Although all optimization techniques themselves are self-navigated, many of them still need an appropriate starting point (initial set of spectral parameters) for optimization to converge. Since optimizations have to be rerun for several times to check for convergence, accuracy as well as uniqueness of a solution, this procedure may involve a substantial role and time-cost of a spectroscopist. Stochastic population-based optimization can overcome this problem, since it processes a population of candidate solutions. Therefore it enables completely automatic characterization and at the same time provides solutions that are not biased by the choice of starting points. Our recent work on spectral characterization based on hybrid evolutionary optimization (HEO) makes the determination of spectral parameters accurate and independent from the choice of starting points (Filipič & Štrancar, 2001, 2002).

Due to the stochastic nature of the HEO method, it has to be applied several times to check for the uniqueness of the solutions. However, the probability of finding the real global minimum in a single run is high with HEO, so only a few runs are enough to get one (best-fit) solution. When simple few-domain spectra (e.g., 2 to 4 domains) are fitted, all solutions that possess high goodness of fit are similar, i.e., all sets of the spectral parameters are almost equal (within error estimation). However, when complex spectra are fitted, the multiple runs of the stochastic optimization procedure provide additional solutions, which have similar goodness of fit but different sets of spectral parameters. The probability of finding such (other-than-best-fit) solutions remains high even if HEO is run for 200 times. This suggests that other-than-best-fit solutions should be taken into consideration as well. However, to identify and interpret this large solution space, a new technique for presentation of the solutions is needed.

In this article we propose an approach to describe the lateral heterogeneity of complex membranes by constructing quasi-continuous distributions of EPR spectral parameters from the solutions of the multiple runs of HEO. This "soft" characterization method elucidates the problem of the number of spectral components and provides a unique method for exploring the lateral heterogeneity of the biomembranes. The properties of the distribution functions of EPR spectral parameters were inspected when characterizing EPR spectra of membranes of DPPC liposomes and horse neutrophils.

Materials and Methods

Material Preparation

DPPC Liposomes

Pure DPPC membranes were prepared in the form of multilamellar liposomes. 50 mg of dry lipids (obtained from Avanti Polar Lipids, Birmingham, AL) were dissolved in 3 ml of chloroform and 1 ml of diisopropylether. The organic solvents were evaporated on a rotary evaporator in a glass flask forming lipid film. One ml of phosphate buffer saline (PBS; 290 mOsmol/kg, pH 7.4) was added to the flask. The suspension was hand-shaken and sonicated for 15 min.

Horse Neutrophils

Neutrophils were taken from bronchoalveolar fluid (BAL) from healthy horses and horses suffering from the chronic obstructive pulmonary disease (COPD), known under different synonyms as asthma-like syndrome. Healthy horses and the ones with COPD were sedated with medetomidine purchased from Domosedan (Turku, Finland). A 2.5-m long endoscope was introduced through the pre-cleaned and topically anesthetized nostril and advanced until it wedged in a bronchus. 300 ml of pre-warmed sterile physiological saline solution was infused through the biopsy channel into the bronchus and immediately re-aspirated into a sterile flask cooled in ice. Polymorphonuclear leukocytes were isolated from whole BAL samples.

EPR Measurements

An appropriate volume of 10^{-4} M solution in ethanol of lipophilic spin probe, methyl ester of 5-doxyl palmitate MeFASL(10,3) (nitroxide radical), was added to the glass tube. A thin film of spin probes deposited on the walls of the glass tube was formed by evaporation of ethanol. To the tube the prepared material was added. The tube was then stirred for 10 minutes and in the case of neutrophils centrifuged for 5 min at $100 \times g$. The labeled sample was transferred into a quartz-glass capillary (1 mm inner diameter) and the EPR spectrum was recorded on a Bruker ESP 300E spectrometer (Karlsruhe, Germany) with microwave frequency of 9.59 GHz and power of 20 mW, modulation frequency of 100 kHz and amplitude of 0.5 G. If needed, the spectra were accumulated over several scans in order to gain the signal-to-noise ratio S/N (typical values for S/N were 150–250).

The Spectrum Simulation Model

Generally, to describe EPR spectra of spin probes, the stochastic Liouville equation is used (Robinson et al., 1985; Schneider & Freed, 1989; Budil et al., 1996). In a membrane system, labeled with doxyl-fatty-acid spin probes and measured at physiological temperatures, the majority of the rotational motions are fast with respect to the EPR time scale. Therefore, the simplification to the restricted fast-motion approximation is physically justified. However, it is possible that the proposed model will not cover the molecular motions at lower temperatures and/or of some spin probes that exhibit slower (''intermediate slow'') motion. In such case the slow motional spectral components could be misinterpreted as restricted fast motional components with high values of order parameter and broadening constant, but low value of rotational correlation time. Consequently, the used spectrum-simulation model will empirically describe the slow motional spectral component as a highly restricted one. Although, the model is not able to cover the full range of possible motions, we believe that, especially for the spectra taken at physiological temperatures for the doxyl-fatty-acid spin probes, the benefits in terms of time-cost justify the use of fast-motion approximation. This concept is therefore a compromise between accuracy of the physical model and low time-cost of the characterization, which enables the characterization to be performed on a PC computer.

Since the approach has been already discussed elsewhere (Schindler & Seelig, 1973; Štrancar, Šentjurc & Schara, 2000), it is only revised here. In the model it is taken into account that the spectrum is composed of several spectral components, which are described with different sets of spectral parameters and reflect different environments of the spin probe. The calculation of every spectral component involves three calculation steps. In the first step, the magnetic interaction tensors are averaged over fast stochastic restricted rotational motions of the nitroxide spin probes to calculate the resonant field distribution (Van, Birrell & Griffith, 1974; Griffith & Jost, 1976). This is done according to the order parameter, S, for the assumed averaged orientation of the nitroxide group relative to the membrane normal vector. The use of a scalar order parameter limits the model application to the experiments, which involve fatty-acid spin probes, physiological temperatures and systems that do not exhibit strong rotational restrictions to axial rotation of the spin probes. This last approximation is fulfilled if the concentration of cholesterol or other rigid membrane constituents is low. In the same calculation step, the polarity correction factors p_A and p_g are used to describe the effect of the neighboring electric fields (including effect of polarity) that influence the electron-density distribution of the spin-probe molecules (Marsh, 1981). The second step includes derivation of the Lorentzian linewidths where the motional narrowing approximation (Nordio, 1976) is used. Two parameters are applied: the rotational correlation time τ_c, and the broadening constant W. τ_c describes the effective rate of motion; for the sake of smaller error only one rotational correlation time is used. W arises primarily due to unresolved hydrogen superhyperfine structure together with minor paramagnetic impurities (e.g., due to usually present oxygen), external field inhomogeneities, and modulation effects, which are about the same for all domain types. But particular domain types could differ in the line broadening due to high spin-label concentration or anisotropy of spin-label motion. In the third step, the convolution of the resonant field distribution with the first derivative of the lineshape is calculated for all spectral lines. The proportions of a particular spectral component are taken into account according to the weighting factor (proportion) d. The result of the convolution is the lineshape of the simulated EPR spectrum. This procedure is implemented in the software EPRSIM Version 4.9 (© Janez Štrancar, 1996-2003; http://www2.ijs.si/~jstrancar/software.htm).

EPR Spectral Decomposition and Optimization

The described procedure allows us to decompose a spectrum $I(B)$ into a different number N_d ($N_d \leq 5$) of spectral components $I_i(B)$ described by different spectral parameters:

$$I(B) = \sum_{i=1}^{N_d} I_i(B) d_i, \tag{1}$$

where B is a magnetic field, i is the spectral component index, d_i, is the proportion of individual spectral component ($\sum_{i=1}^{N_d} d_i = 1$) By the given values of spectral parameters, the model produces a simulated EPR spectrum.

Using the proposed simulation model we have to optimize the spectral parameters to find a set that produces the best-fit simulated spectrum. To navigate the optimization, an objective fitting function is introduced. It measures the goodness of fit of the simulated spectrum with the experimental one. The measure is the reduced χ^2, i.e. the sum of the squared residuals between the experimental and simulated spectra divided by the squared standard deviation of the experimental points σ, and by the number of points in the experimental spectrum N (in our case, $N = 1024$):

$$\chi^2 = \frac{1}{N} \sum_{j=1}^{N} \frac{(y_j^{exp} - y_j^{sim})^2}{\sigma^2}. \tag{2}$$

The standard deviation σ is assessed numerically from the points in the simulated spectrum regions where the derivatives are close to zero. This is usually at both ends of the spectrum.

Since we deal with a large number of spectral parameters, an evolutionary optimization method, such as HEO was used (Filipič

& Štrancar, 2001, 2002). The HEO belongs to the class of the stochastic and population-based optimization algorithms. It uses a population of spectral parameter sets (''individuals''; usually 200 or 300), which are optimized at the same time. This type of optimization is described in details elsewhere (Goldberg, 1989). The basic scheme of an optimization loop of an evolutionary algorithm consists of selection of parameters of some spectra from the population, application of the genetic operators such as crossover, mutation and ''directed mutation'' (local optimization such as Simplex Downhill), which generate an ''offspring'' generation, and replacement of the ''parent'' population by the better part of an ''offspring'' population randomly. The combination of the genetic algorithm and local search based on Downhill Simplex enables HEO to find promising regions of solutions and at the same time to extract fine-tuned solutions (Filipič & Štrancar, 2001, 2002). Random generation of the starting population eliminates human navigation from spectral characterization and enables the automation of the whole procedure. Moreover, the stochastic nature of the HEO routine makes it possible to control the complexity of the solution-space and appropriateness or limitations of the simulation model. At the same time it allows us to determine the errors of the spectral parameters independently of the procedure, which involves the covariance matrix analysis. The described optimization method is implemented in EPRSIM 4.9.

Characterization of Membrane Lateral Heterogeneity

Standard Characterization Method

The standard characterization of the EPR spectra resolves a discrete picture of lateral membrane heterogeneity by spectral decomposition. The number of spectral components N_d has to be chosen in advance. All the information is obtained only from the best-fit solution. The HEO routine must be performed several times to achieve appropriate statistics. Running this procedure for M times enables us to choose the best fit from M best fits provided by M runs of the HEO. Obtained parameters can be summarized in a table (N_d sets of parameters) and simple graphs. Since only the best fit is used, all additional information from other-than-best-fit solutions, which may give us some hints about the appropriateness of the simulation model or about the unresolved complexity of the solution, are neglected.

Soft Characterization Method

In general, when the number of spectral components diverges, we should speak about a continuous picture of lateral membrane heterogeneity instead of the discrete one. If exact parameterization of the complex spectra in the continuous picture could be obtained, one would deal with the distribution of spectral component proportions over various spectral parameters. Such distribution will be referred to as ''original distribution''. The distribution, which includes few major spectral components and lots of minor spectral components, will be denoted as ''quasi-continuous'' original distribution. The term ''major'' component indicates a spectral component with a significant proportion and at the same time a component found by the majority of HEO runs. Since we also want to detect ''minor'' spectral components, i.e., the quasi-continuous distribution, the approach will be referred to as ''soft'' characterization method.

Let us suppose that the EPR spectrum of a complex membrane can be described similar to Eq. 1

$$I(B)^{\mathrm{orig}} = \sum_{i=1}^{N_d^{\mathrm{orig}}} I_i(B) d_i, \tag{3}$$

whsere N_d^{orig} is the number of spectral components arising from the existing membrane heterogeneity. It is then expected that the standard method can be successfully applied when the number of fitted spectral components N_d is equal or higher than N_d^{orig}. However, when N_d^{orig} is high, the choice of an arbitrarily high N_d would make the procedure too slow and inefficient. On the other hand, N_d should not be lower than the number of major spectral components. Therefore, $N_d = 4$ seems to be an appropriate choice, since it is higher than the usual number of domain types used for describing membrane heterogeneity but it is still not too large.

The soft-characterization method differs from the standard method only in collecting and presenting the solutions. In contrary to the standard-characterization method, M best fits of M runs are used instead of only the best one. Because we are interested in motional and polarity characteristics, deduced from each spectral component i ($i = 1, \ldots, N_d$) of each run m ($m = 1, \ldots, M$), the following spectral parameters will represent the ''fast-motion approximation basis set'': order parameter $S_{i,m}$, spectral component proportion $d_{i,m}$, rotational correlation time $\tau_{c,i,m}$, broadening constant $W_{i,m}$, and hyperfine polarity correction $p_{A,i,m}$. Since the large number of HEO runs had to be implied (M in the order of hundreds), a large amount of data, i.e., $M \times N_d$ sets of 5 parameters, emerges. To present this data, a special compact form of presentation is used. All M best-fit solutions with N_d spectral components are presented together, resulting in a pattern mimicking the original distribution of proportions.

In Fig. 1, the construction of this distribution is demonstrated. The synthetic spectrum is presented, which is constructed from 15 spectral components. In Fig. $1A_1$ EPR spectra of these spectral components are plotted with the intensity corresponding to the appropriate proportions and at positions corresponding to the order parameters of individual spectral components. The scale for the order parameter in Fig. $1A_1$ is the same as in Fig. $1A_2$, where the distribution of spectral component proportions is plotted against order parameter. This distribution should be considered as ''original distribution''. When searching for this ''original distribution'', lots of equivalent projections (solutions of different HEO runs) are found with the proposed number of spectral components $N_d = 4$. In Fig. $1B_1$ four such solutions (fits to the spectrum constructed of components shown in Fig. $1A_1$) are presented in the same way as the components in Fig. $1A_1$. To search for the original distribution we plot the proportions of individual spectral components of all solutions against the order parameter. In such a way, the distribution-like pattern in Fig. $1B_2$ is constructed. To find the best approximation of the original distribution one has to perform several (hundreds of) runs. Since all spectral simulations are performed within the model characterized by N_d spectral components (for example, $N_d = 4$), it is assumed, that each optimization run provides an N_d-dimensional projection of the original distribution (4-dimensional projection or shortly denoted as *4D-projection*).

If the original distribution is continuous, any proposed number of spectral components N_d applicable within the simulation model is smaller than the original number of spectral components N_d^{orig}. Therefore the fitting function χ^2 of any solution could not reach the theoretical limit of 1. At the same time, many N_d projections can have similar χ^2. They are referred to as equivalent projections; χ^2-equivalent but parametrically different solutions. To find them, the HEO routine is used due to the features already discussed (stochastic, genotype-driven, etc.) (Goldberg, 1989).

In order to present any kind of distribution-like patterns, the parameter over which the distribution is to be determined should be chosen. The appropriate parameter to classify the spectral

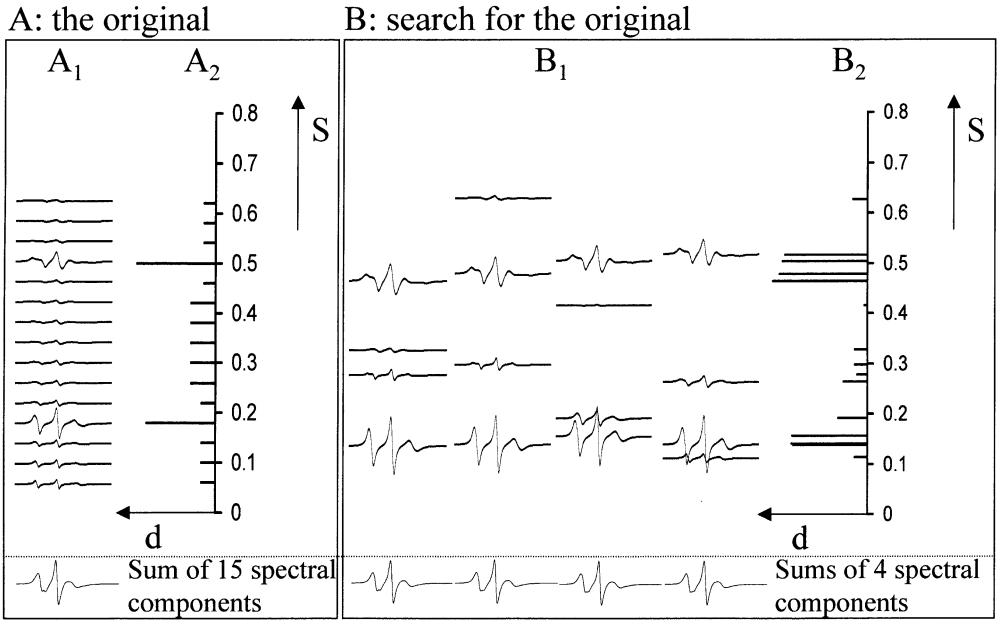

Fig. 1. A schematic presentation of the construction of a distribution of spectral component proportions against the order parameter S in the soft characterization method. (A_1) Fifteen original spectral components (center field 0.342 T, sweep 0.01 T) composing a (2+13)-D spectrum are plotted with the intensity corresponding to appropriate proportions and at positions corresponding to the order parameters S of particular spectral components. The sum of these 15 spectral components is shown at the bottom. (A_2) The distribution of spectral component proportions d plotted against order parameter. This distribution is considered as the "original distribution". (B_1) Four of the equivalent 4-D projections—solutions of different HEO with $N_d = 4$—of the spectrum constructed from components (center field 0.342 T, sweep 0.01 T) shown in A_1, presented in the same way as the components in A_1. Sums of 4 spectral components are shown at the bottom. (B_2) The distribution-like pattern is constructed from the mentioned 4 equivalent projections by plotting the proportions d of individual spectral components of these 4 solutions against the order parameter S.

component i of a solution m seems to be the order parameter $S_{i,m}$, because the goodness of fit is the most sensitive just to the order parameter. To present the proportion of each spectral component and to take into account the goodness of fit χ^2_m of solution m as well as the repeatability in terms of spectral component density $\rho(S_{i,m})$, the transformed proportions $d^*_{i,m}$ will be shown. The spectral component density $\rho(S_{i,m})$ measures the repeatability of HEO-found spectral components at various order parameters $S_{i,m}$, counted within the grid $\Delta S = 8/(M \times N_d)$. This assumes that an average density within one grid cell is 8 counts, as would be expected for a random distribution of order parameters over the entire interval for $M = 200$ and $N_d = 4$. The transformation of $d_{i,m}$ to $d^*_{i,m}$ is therefore defined through

$$d^*_{i,m} = d_{i,m} \times \exp\left[-\frac{1}{2}\left(\frac{\chi^2_m - \chi^2_{min}}{\sigma_{\chi^2}}\right)^2\right] \times \exp\left[-\frac{1}{2}\left(\frac{\sigma_\rho}{\rho(S_{i,m})}\right)^2\right] \quad (4)$$

with χ^2-filter width σ_{χ^2} and density-filter width σ_ρ. The value of χ^2-filter width σ_{χ^2} is chosen in such a way that the interval (χ^2_{min}, $\chi^2_{min} + \sigma_{\chi^2}$) includes 66% of all solutions. This limit was determined empirically and is discussed in the Results section. The second value, σ_ρ defines the significance level of spectral component density, chosen to be equal to 5 counts per grid cell. The proposed transformation assures that the proportions of spectral components, which correspond to most-favorable fits, will remain almost unchanged. On the contrary, the less-favorable fits that possess much higher values of the fitting function χ^2 compared to χ^2_{min}, as well as those solutions that have low spectral component density ρ, are diminished.

In all the presentations, transformed proportions $d^*_{i,m}$ are plotted against order parameters $S_{i,m}$, where the spectral component i of the solution m is presented with a thin vertical bar of height, which corresponds to $d^*_{i,m}$, at the position of $S_{i,m}$. In addition, if more information about the solution in terms of the other three spectral parameters ($\tau_{c,i,m}$, $W_{i,m}$, and $P_{A,i,m}$) is desired, it can be presented in terms of color of a particular bar. The color of each bar can be defined through the RGB specification where the intensity of each color component (red, green, and blue, respectively) represents the relative value of the parameters $\tau_{c,i,m}$, $W_{i,m}$, and $P_{A,i,m}$ respectively (*see* the "calibration cube" shown in Fig. 3 legend). This enables us to present additional three dimensions. Combining the 2-dimensional presentation described above and the coloring of the bars, we are therefore able to compactly present a 5-dimensional data structure. Here it should be stressed that the RGB presentation is not sensitive to small-parameter variations. Consequently, parametrically similar spectral components will be presented with similar colors, enabling classification of a group of spectral components as a particular domain type. This would not be possible if the coloring would be too sensitive to small parameter changes.

Since different colors correspond to different characteristics (rate τ_c, anisotropy of motion and spin label concentration W, as well as polarity p_A) this presentation can help to explore the complex domain structures. It enables us to monitor the changes in the proportion distributions as well as the properties of each solution when the system is exposed to different modification or external stress conditions. From now on the presentation of soft characterization will be referred to as *colored distribution of EPR spectral parameters* (CODE).

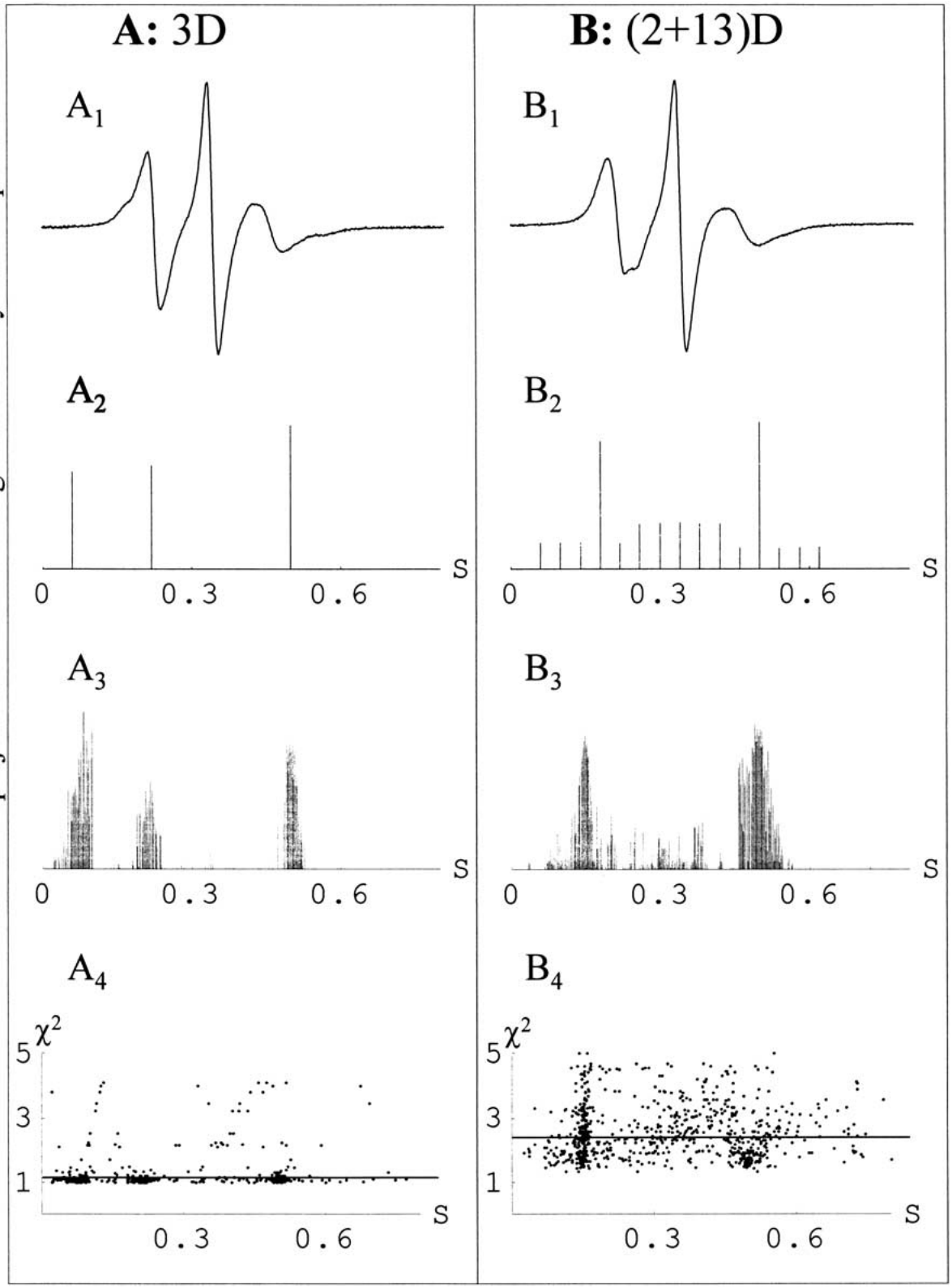
A: 3D
B: (2+13)D
Synthetic Spectrum
original
4D-projection
A1
B1
A2
B2
A3
B3
A4
B4
S
0
0.3
0.6
χ2
5
3
1

Fig. 2.

Fig. 2. (A_1) A synthetic 3-D spectrum composed of three spectral components (center field 0.342 *T*, sweep 0.01 *T*). (A_2) The original distribution of proportions of three spectral components against the order parameter *S* from which the 3-D spectrum is constructed. (A_3) The result of multiple runs of HEO: the discrete-like distribution of proportions of spectral components against the order parameter *S*. The width of each apparent group of determined spectral components represents its standard deviation and includes the statistical error due to spectral noise as well as the systematic error due to the stochastic optimization. (A_4) The χ^2-distribution of spectral components of all solutions of multi-run HEO plotted against the order parameter *S*. Each point represents the spectral component with appropriate order parameter *S* and χ^2. The χ^2-filter upper limit is represented with the horizontal line, below which 66% of points with lower χ^2 lie. (B_1) Synthetic (2+13)-D spectrum composed of 15 spectral components (center field 0.342 *T*, sweep 0.01 *T*). (B_2) The original distribution of 2 major spectral components (with high proportion) and 13 minor ones (with small proportion), from which the synthetic (2+13)-D spectrum is constructed. (B_3) The result of multi-run HEO: the continuous-like distribution of proportions of spectral components plotted against the order parameter *S*. (B_4) The χ^2-distribution of spectral components of all solutions of multi-run HEO plotted against order parameter *S*. The χ^2-filter upper limit was determined similarly as in Fig. 2A_4. The number of runs in each characterization procedure was 200.

RESULTS

Establishment of Soft Characterization on Synthetic Spectra

In order to establish the soft approach to the lateral heterogeneity picture, we made several numerical experiments, which involved multi-run optimizations on synthetic spectra with predefined spectral parameters. The spectra were calculated within the simulation model introduced previously. The number of runs in each characterization procedure was $M = 200$ to gain the resolution.

To assure that this approach does not generate solutions with spectral components, which cannot be found in the original distribution, we first performed optimizations of the spectral parameters of a synthetic 3-D spectrum (Fig. 2A_1). This spectrum is constructed from three spectral components shown in the original distribution (Fig. 2A_2). The predefined number of spectral components within the characterization procedure was $N_d = 4$. The multi-run HEO optimization gives three spectral components in the discrete-like distribution of calculated spectral components against the order parameter in Fig. 2A_3. The width of each apparent group of determined spectral components represents its standard deviation and includes the statistical error due to spectral noise as well as the systematic error due to the stochastic optimization. It can be seen in Fig. 2A_3 that the soft characterization method does not generate additional solutions with respect to the original distribution. Although the procedure was allowed to find four arbitrary spectral components (since $N_d = 4$), CODE revealed three (Fig. 2A_3), which is the same as in the original distribution (Fig. 2A_2). This indicates that the proposed method does not overfit spectra. Since we do not have a continuous distribution of spectral components, this represents a case where also the standard characterization method could be used.

In addition, the χ^2 Distribution of components of all solutions against order parameter is shown in Fig. 2A_4. Each point represents the spectral component with appropriate order parameter and with χ^2 that equals the χ^2 of the corresponding solution. The points with lower χ^2 values (good solutions) nicely resolve a discrete-like distribution, i.e., all three major spectral components are found. From comparison of Fig. 2A_3 and Fig. 2A_4 it can be seen that the points with higher χ^2 values do not represent appropriate solutions. Therefore they should be filtered out by the χ^2-filter (explained in the previous section). In the same figure, Fig. 2A_4, the χ^2-filter upper limit is represented with the horizontal line. Below the line, there are 66% of points with lower χ^2. Moreover, it can be seen that the spectral component density is high only at order parameter values that are close to order parameters of spectral components of the original distribution. Other points where the density is much lower should be filtered out by the density filter (explained in the previous section).

In the second case, the (2+13)-D spectrum (Fig. 2B_1; already shown in Fig. 1*A*) is constructed from two major components and thirteen minor ones. As it was already described in a previous section, the terms "major" and "minor" refer to the proportions of the spectral components. The large number of minor components emulates a quasi-continuous spectral-component distribution (Fig. 2B_2). In Fig. 2B_3 the result of multi-run HEO with $N_d = 4$ (4-D projection) is shown. The two major components are obtained successfully. Moreover, also the majority of minor components (with smaller proportions) are found. It can be seen in Fig. 2B_4 that the χ^2 distribution is much more dispersed than the χ^2 distribution shown in Fig. 2A_4. The higher χ^2 values arise mainly do to inability of the simulation model with $N_d = 4$ to simulate spectra composed of more spectral components than N_d. At the same time the spectral component density was found to be much more uniform than in the problem presented in Fig. 2A_4. This indicates that the multi-run HEO finds many equivalent and at the same time statistically significant solutions within the proposed simulation model, which can then be represented to give a quasi-continuous distribution. Similarly as in Fig. 2A_4, the χ^2-filter upper limit is represented with a horizontal line, below which 66% of points with lower χ^2 lie.

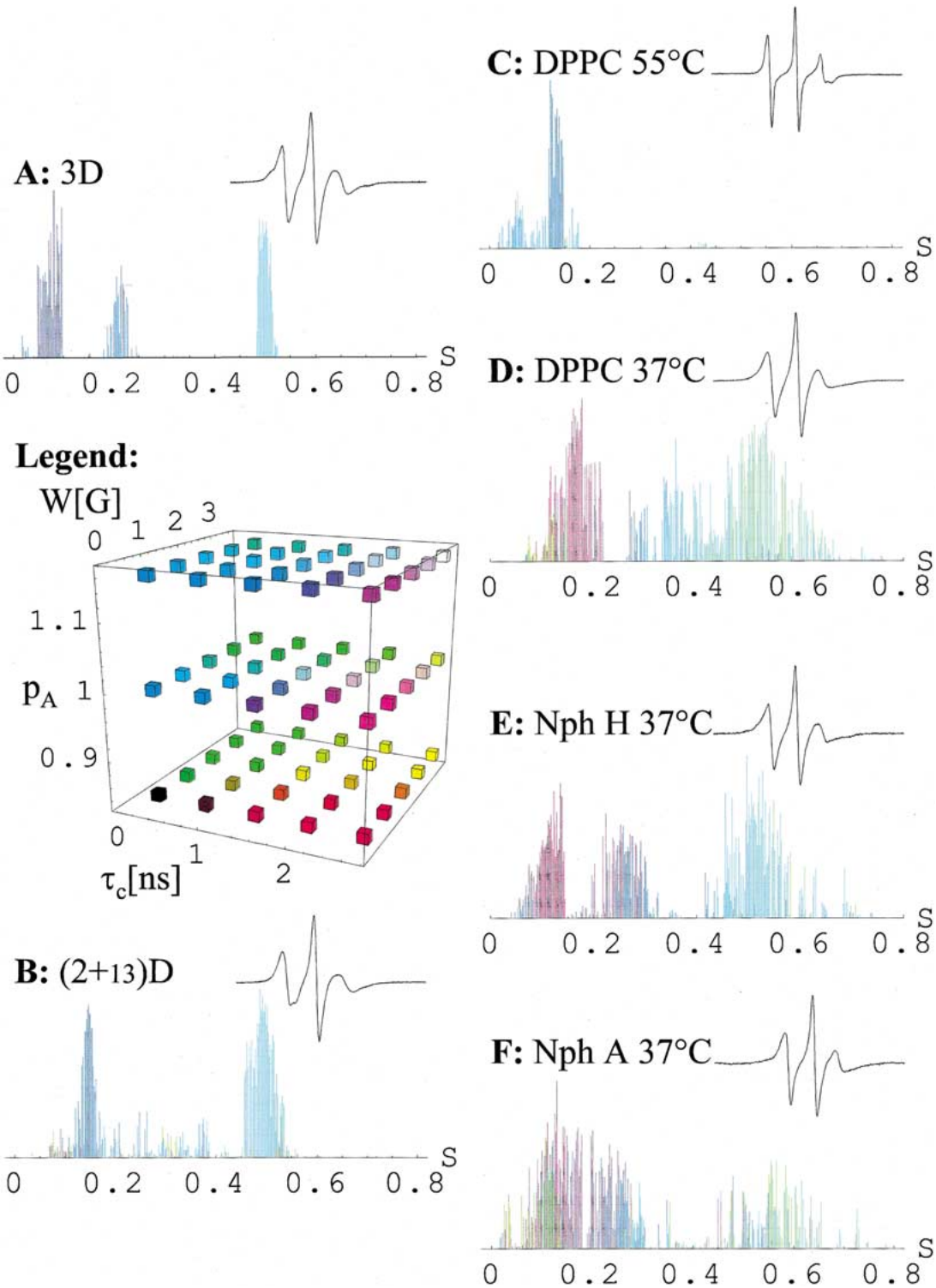

Fig. 3. EPR spectra (center field 0.342 *T*, sweep 0.01 *T*) and corresponding CODEs of the following samples: (*A*) synthetic 3-D; (*B*) synthetic (2+13)-D; (*C*) DPPC liposomes at 55°C; (*D*) DPPC liposomes at 37°C; (*E*) neutrophils from bronchoalveolar fluid of a healthy horse—*Nph H*—at 37°C; (*F*) neutrophils from bronchoalveolar fluid of an asthmatic horse—*Nph A*—at 37°C. All experimental samples were spin-labeled by MeFASL(10,3). The number of HEO runs in each characterization procedure was 200. (*Legend*) The color of a bar in a CODE is defined by the RGB specification where the intensity of each color component (red, green, and blue, respectively) represents the relative value of the spectral parameters: the rotational correlation time τ_c from 0 to 3 ns, the broadening constant *W* from 0 to 0.0003 *T*, and the hyperfine polarity correction p_A from 0.8 to 1.2.

The combination of problems such as 3-D and (2+13)-D was used to tune the filter widths in order to detect the quasi-continuous distribution and at the same time to eliminate solutions that possess lower goodness of fit and lower densities. The 3-D problem requires more restricted χ^2-filtering and density-filtering. On the contrary, the (2+13)-D problem requires just the opposite, since the dispersion of points can report about the quasi-continuous distribution which can possibly exist in the spectra. Therefore we tuned both filter widths to enable detection of discrete and quasi-continuous distributions at the same filter-width values. The resulting filter-width values are 66% for χ^2-filtering and 5 for density-filtering.

Soft Characterization of Liposomes

Firstly, the soft characterization technique was applied to the membranes of pure DPPC liposomes labeled with MeFASL(10,3). An EPR spectrum recorded at 55°C (Fig. 3*C*), which is approximately 13°C above the main transition between the gel lipid phase and the fluid disordered lipid phase (Heimburg, 1998), was characterized in order to check whether the proposed approach reports fluid disordered phase. In the CODE (Fig. 3*C*), one major peak of spectral components with low order parameter and additional spectral components with much smaller proportions and even lower order parameter can be seen. The spectral components in the CODE are characterized by the rotational correlation time τ_c around 1 ns, the hyperfine polarity correction p_A is greater than 1, whereas the broadening constant W is small enough to confirm low local concentration of spin probe molecules and negligible anisotropy of motion. The CODE of DPPC liposomes at 55°C therefore reveals fluid membrane structure, as it is expected from the literature (Vist & Davis, 1990).

On the other hand, the spectrum of the same sample at 37°C (Fig. 3*D*) was also recorded to check how the method describes the coexistence of lipid phases expected at 37°C, i.e., between the main transition at 42°C and the pre-transition at 35°C for DPPC (Tsuchida & Hatta, 1988; Mouritsen & Jørgensen, 1994). It can be seen from Fig. 3*D* that there are two major broad peaks of spectral components, one with the order parameter S around 0.5 and the other with S around 0.15. This CODE reveals slower motion at a rate of 2 ns for the group of less ordered (*violet*) spectral components, but faster motions for the spectral components with S around 0.5 (*light green*) and spectral components with S around 0.35 (*light blue*). Moreover, the light green spectral components correspond to higher W, which indicates that local concentration of spin probes could be higher in that domain type or that the anisotropy of motion is no more negligible.

Soft Characterization of Biomembranes

Although the soft characterization was established on many numerical experiments on the synthetic spectra and the spectra of liposome membranes, the main emphasis should be on the application of this method for the biomembrane complexity characterization. Consequently, we want to show in this section the benefits of the soft characterization method on the spectra of biomembranes, i.e., spin-labeled membranes of horse neutrophils. The number of runs in each characterization procedure was again $M = 200$. The aim is to compare the CODEs of liposomes and neutrophils, as an example of increased compositional complexity, and neutrophils from bronchoalveolar fluid of the healthy horses and of those with asthma-like disease, as an example of different physiological conditions.

As it can be seen from the CODE characterization of membranes of healthy neutrophils (Fig. 3*E*), these membranes possess more discrete-like domain structure in contrast to liposome membrane from pure DPPC at the same temperature (Fig. 3*D*). Another interesting detail can be seen in the broad peak of spectral components at S around 0.5 in the case of healthy neutrophils (Fig. 3*E*), which, in fact, consists of two groups of spectral components–domain types. The blue domain type has a large polarity correction factor p_A, but not very high τ_c and W. The yellow-green domain type has low p_A, low τ_c and high W. This result points to the existence of two different domain types with similar anisotropy of rotational motions but with different accessibility to water (different p_A) and local concentration of spin probe (different W). Similarly, the broad peak of spectral components around $S = 0.3$ also consists of two different domain types (the *violet* and the *dark blue*), which possess similar S and p_A but differ in τ_c and W. The dark blue domain type has τ_c below 1 ns, while the violet domain type has τ_c around 2 ns. Therefore, the CODE in Fig. 3*E* shows at least 5 different domain types. This clearly indicates that the healthy horse neutrophils' membrane has a more complicated structure than the DPPC membrane, while the characterization of the DPPC liposome membrane reveals no different solutions at similar S (Fig. 3*D*). On the other hand, in the case of the DPPC liposomes, the distribution of the spectral components over S is more continuous-like.

When comparing neutrophil cells of healthy (*Nph H*) and asthmatic (*Nph A*) horses, a difference is evident in the complexity of the two samples. The *Nph A* sample (Fig. 3*F*) shows a considerably larger proportion of less-ordered domains compared to the *Nph H* (Fig. 3*E*). The well-defined discrete distribution of the spectral components (less-ordered domains) in the case of the *Nph H* has changed into almost continuous distribution in the case of the *Nph A*. Careful analysis of the two CODEs (Fig. 3*E* and 3*F*) reveals some additional in-

teresting differences between the two samples. Firstly, the expressed group of blue spectral components at high values of S (ordered domain with large p_A but not very high τ_c and W) disappears from the spectrum of the *Nph A* sample. This leads to the conclusion that the *Nph A* in contrast to the *Nph H* do not possess the ordered domains with high accessibility to water. Moreover, a new domain type can be found in the *Nph A*, according to the appearance of green spectral components at very low S (less-ordered domain with high W, low p_A and τ_c around 1 ns). With respect to high W, this domain type accepts a high local concentration of spin probes. One can speculate that this domain type was transformed from a part of the violet domain type, i.e., from less-ordered spectral components with high τ_c to less-ordered spectral components with very low τ_c.

Discussion

It is known that sphingolipids, cholesterol, peptides and larger proteins, as well as phospholipids with saturated or nonsaturated acyl chains, can influence the motional properties of surrounding molecules and by doing so can influence the formation of different domain types (Welti & Glaser, 1994). Consequently, complex EPR spectra can occur when the compositional complexity of a membrane is increased or when physiological conditions affecting the membrane, change. Therefore a real biomembrane (rich in different membrane constituents) can consist of several different domains with different motional characteristics (Glaser, 1993; Edidin, 1997), which induces many different spectral components in EPR spectra. Relatively large domain walls (compared to the size of an individual domain) with continuous variation of motional characteristics could also increase the level of complexity. For that reason, we believe that the soft characterization method, which allows a large number of different lateral domain types, is needed to study the lateral heterogeneity of biomembranes.

As it was established on the synthetic 3-D spectrum and $(2+13)$-D spectrum (Fig. 2), the soft characterization method is tuned to resolve discrete as well as quasi-continuous distributions of spectral components. Since all spectral optimizations are performed within the model characterized by N_d spectral components, it is assumed that each optimization run provides an N_d-dimensional projection of the original distribution of spectral components (spectral parameters). At the same time the use of stochastic hybrid evolutionary optimization (HEO) guarantees that these different (but χ^2-equivalent) solutions can be found.

The result of the soft characterization of the liposome membrane proves the relative simplicity of the liposome membrane composed from single lipid species at the temperature far above the main transition (Fig. 3*C*). However, at 37°C a broad peak of spectral components at higher-order parameter S was found (Fig. 3*D*). Even though this is a pure DPPC membrane, it is measured close to the temperature of phase transition between different lipid phases, so it is possible that the phase separation occurs, while only one type of phospholipid molecules is present in the membrane (Mouritsen & Jørgensen, 1994). We might speculate that the detected broad peak distribution of spectral components could originate from the domain walls. Nonetheless, it can be concluded that even for the DPPC liposome membrane at 37°C the standard (discrete) characterization method for describing the lateral membrane heterogeneity may not be accurate enough, although it seems that the standard method is an appropriate choice at many temperatures (e.g., *see* Fig. 3*C*) and under other conditions.

The CODEs of the membranes of neutrophil cells of healthy and asthmatic horses (Fig. 3*E* and 3*F*, respectively) provide a more complex picture of lateral membrane heterogeneity. Additionally, the differences between the CODEs of *Nph H* (Fig. 3*E*) and *Nph A* (Fig. 3*F*) clearly indicate altered lateral membrane heterogeneity. Namely, in the case of *Nph A*, a new domain type emerges for the order parameter S around 0.1 (less-ordered domains with fast rotational motions, low accessibility to water and high spin-probe concentration). Moreover, one domain type disappears at order parameter around $S = 0.5$ (ordered domain types with fast rotational motions, high accessibility to water and low spin-probe concentration). Finally, the smeared distribution of slow and less-ordered domains in the case of *Nph A* also indicates that the membrane lacks some of the active systems that otherwise maintain a "supervised" membrane lateral heterogeneity structure.

At the end, it should be stressed that the complexity in the lateral heterogeneity picture does not necessarily originate only from complex biochemical composition and lipid phase separation, but also from membrane active elements, larger domain walls, different membranes in single cells (when measuring suspensions of cells), biological diversity among the cells, as well as from vertical distribution ("instability") of the spin probes.

It should not be overlooked that the domain picture depends on the experimental method used and is therefore determined by its time and distance scales. Therefore every method would strongly need an additional experimental support from other experimental methods as well as computational methods. In order to detect the complexity in the lateral domain structure of a membrane, the method has to have a near-molecular resolution and at the same time possibility to examine larger membrane systems (the last is still challenging for the molecular dynamic simulation methods). Currently such additional in-

formation cannot be obtained by other methods. Hence, we believe that the presented approach of the soft characterization provides a powerful tool of membrane lateral heterogeneity characterization and should be used by the experimentalist to systematically resolve the adaptation of membranes caused by different stress or pathological conditions. However, one must be aware of the limitations of this method imposed by the use of restricted fast-motion approximation, which only empirically describes slow motional spectral components (if they are present) as highly restricted fast motional components.

Conclusions

In biomembranes a complex level of lateral heterogeneity is expected due to the complex lipid composition, embedded proteins, and macromolecular structures such as cytoskeleton and glycocalyx, which are expected to affect the lateral domain structure and to widely increase its complexity. In this work it was shown that an insight into the lateral heterogeneity of membranes could be obtained by an appropriate interpretation of EPR spectra of spin-labeled lipid bilayers. We have demonstrated that the new approach of interpreting EPR spectra introduced in this work, i.e., the soft characterization method, can be successfully used to gain at least qualitative insight into the lateral heterogeneity of biomembranes. A special presentation technique, CODE, was introduced, which allows a compact presentation of a large amount of data that characterize different domain types and distributions of their properties. It was shown that in many cases discrete distributions of properties of membrane domains are not appropriate and that reliable results can be obtained only by construction of a continuous distribution of domain-type properties. Besides motional characteristics of domains also data about the polarity of the spin-label environment in particular domain types, as well as estimation about the non-uniformity of spin-label distribution between the domains can be obtained.

The most important step in this work was the application of projections to reveal continuous distributions of spectral parameters of corresponding spectral components, which was made possible by the use of HEO. Therefore, the soft characterization and CODE provide a possibility to study complex lateral heterogeneity in biomembranes (within the presented model) with some insight into the membrane domain characteristics, which in our opinion are not available by other methods.

This work was carried out with the financial support of the Ministry of Education, Science and Sport of the Republic of Slovenia. Special thanks to Prof. Bogdan Filipič from the Department of Intelligent Systems of the "Jožef Stefan" Institute (Ljubljana, Slovenia) for much advice in terms of expert knowledge in the field of evolutionary optimization; to Prof. Zlatko Pavlica from the Veterinary Faculty (University of Ljubljana, Ljubljana, Slovenia) for isolation and preparation of horse neutrophil samples, as well as to Prof. Marcus A. Hemminga from the Laboratory of Biophysics (Wageningen University, Wageningen, The Netherlands), and to Prof. Milan Schara and Dr. Marjeta Šentjurc from the Department of Solid State Physics ("Jožef Stefan" Institute, Ljubljana, Slovenia) for helpful and critical discussions.

References

Arsov, Z., Schara, M., Štrancar, J. 2002. Quantifying the lateral lipid domain properties in erythrocyte ghost membranes using EPR-spectra decomposition. *J. Magn. Reson.* **157**:52–60

Bloom, M., Thewalt, J.L. 1995. Time and distance scales of membrane domain organization. *Mol. Membr. Biol.* **12**:9–13

Budil, D.E., Lee, S., Saxena, S., Freed, J.H. 1996. Nonlinear-least-squares analysis of slow-motion EPR spectra in one and two dimensions using a modified Levenberg-Marquardt algorithm. *J. Magn. Reson. A* **120**:155–189

Chachaty, C., Soulie, E.J. 1995. Determination of electron spin resonance static and dynamic parameters by automated fitting of the spectra. *J. Phys. III* **5**:1927–1952

Della Lunga, G., Pogni, R., Basosi, R. 1998. Global versus local minimization procedures for the determination of spin Hamiltonian parameters from electron spin resonance spectra. *Mol. Phys.* **95**:1275–1281

Devaux, P.F., Seigneuret, M. 1985. Specificity of lipid-protein interactions as determined by spectroscopic techniques. *Biochim. Biophys. Acta* **822**:63–125

Dibble, A.R., Hinderliter, A.K., Sando, J.J., Biltonen, R.L. 1996. Lipid lateral heterogeneity in phosphatidylcholine/phosphatidylserine/diacylglycerol vesicles and its influence on protein kinase C activation. *Biophys. J.* **71**:1877–1890

Edidin, M. 1997. Lipid microdomains in cell surface membranes. *Curr. Opin. Struct. Biol.* **7**:528–532

Eviatar, H., van der Heide, U.A., Levine, Y.K. 1995. Computer simulations of the electron spin resonance spectra of steroid and fatty acid nitroxide probes in bilayer systems. *J. Chem. Phys.* **102**:3135–3145

Filipič, B., Štrancar, J. 2001. Tuning EPR spectral parameters with a genetic algorithm. *Applied Soft Computing* **1**:83–90

Filipič, B., Štrancar, J. 2002. Evolutionary computational support for the characterization of biological systems. *In*: Evolutionary Computation in Bioinformatics. G.B. Fogel, and D.W. Corne, editors. pp. 279–294. Morgan Kaufmann Publishers, San Francisco

Gaffney, B.J., Marsh, D, 1998. High-frequency, spin-label EPR of nonaxial lipid ordering and motion in cholesterol-containing membranes. *Proc. Natl. Acad. Sci. USA* **95**:12940–12943

Ge, M., Field, K.A., Aneja, R., Holowka, D., Baird, B., Freed, J.H. 1999. Electron spin resonance characterization of liquid ordered phase of detergent-resistant membranes from RBL-2H3 cells. *Biophys. J.* **77**:925–933

Glaser, M. 1993. Lipid domains in biological membranes. *Curr. Opin. Struct. Biol.* **3**:475–481

Goldberg, D.E. 1989. Genetic Algorithms in Search, Optimization and Machine Learning. Addison-Wesley, Reading

Griffith, O.H., Jost, P.C. 1976. Lipid spin labels in biological membranes. *In*: Spin Labeling, Theory and Application. L.J. Berliner, editor. pp. 453–523. Academic Press, New York

Heimburg, T. 1998. Mechanical aspects of membrane thermodynamics. Estimation of the mechanical properties of lipid

membranes close to the chain melting transition from calorimetry. *Biochim. Biophys. Acta* **1415**:147–162

Hønger, T., Jørgensen, K., Biltonen, R.L., Mouritsen, O.G. 1996. Activity and Dynamic Lipid Bilayer Microheterogeneity. *Biochemistry* **35**:19–38

Kirste, B. 1992. Methods for automated analysis and simulation of electron paramagnetic resonance spectra. *Anal. Chim. Acta* **265**:191–200

Koklič, T., Šentjurc, M., Zeisig, R. 2002. The influence of cholesterol and charge on the membrane domains of alkylphospholipid liposomes as studied by EPR. *J. Lipos. Res.* **12**:335–352

Loura, L.M.S., Fedorov, A., Prieto, M. 2001. Fluid-fluid membrane microheterogeneity: A fluorescence resonance energy transfer study. *Biophys. J.* **80**:776–788

Marsh, D. 1981. Electron spin resonance: spin labels. *In*: Membrane Spectroscopy. E. Grell, editor. pp. 51–142. Springer-Verlag, Berlin

Marsh, D., Horváth, L.I. 1998. Structure, dynamics and composition of the lipid-protein interface. Perspectives from spin-labelling. *Biochim. Biophys. Acta* **1376**:267–296

Moens, P., De Volder, P., Hoogewijs, R., Callens, F., Verbeeck, R. 1993. Maximum-likelihood common-factor analysis as a powerful tool in decomposing multicomponent EPR powder spectra. *J. Magn. Reson. A* **101**:1–15

Mouritsen, O.G., Jørgensen, K. 1994. Dynamical order and disorder in lipid bilayers. *Chem. Phys. Lipids* **73**:3–25

Nordio, P.L. 1976. General magnetic resonance theory. **In**: Spin Labeling, Theory and Application. L.J. Berliner, editor. pp. 5–51. Academic Press, New York

Percot, A., Lafleur, M. 2001. Direct observation of domains in model stratum corneum lipid mixtures by Raman microspectroscopy. *Biophys. J.* **81**:2144–2153

Rinia, H.A., de Kruijff, B. 2001. Imaging domains in model membranes with atomic force microscopy. *FEBS Lett.* **504**:194–199

Robinson, B., Thomann, H., Beth, A., Fayer, P., Dalton, L.R. 1985. The phenomenon of magnetic resonance: Theoretical considerations. **In**: EPR and Advanced EPR Studies of Biological Systems. L.R. Dalton, editor. pp. 11–110. CRC Press, Boca Raton

Sankaram, M.B., Marsh, D., Thompson, T.E. 1992. Determination of fluid and gel domain sizes in two-component two-phase lipid bilayers: An electron spin resonance spin label study. *Biophys. J.* **63**:340–349

Schindler, H., Seelig, J. 1973. EPR spectra of spin labels in lipid bilayers. *J. Chem. Phys.* **59**:1841–1850

Schneider, D.J., Freed, J.H. 1989. Calculating slow motional magnetic resonance spectra: A user's guide. *In*: Biological Magnetic Resonance: Spin Labeling, Theory and Applications. L.J. Berliner, and J. Reuben, editors. pp. 1–76. Plenum Press, New York

Sok, M., Šentjurc, M., Schara, M. 1999. Membrane fluidity characteristics of human lung cancer. *Cancer Lett.* **139**:215–220

Štrancar, J., Šentjurc, M., Schara, M. 2000. Fast and accurate characterization of biological membranes by EPR spectral simulations of nitroxides. *J. Magn. Reson.* **142**:254–265

Tocanne, J.-F., Cezanne, L., Lopez, A., Piknova, B., Schram,V., Tournier, J.-F., Welby, M. 1994. Lipid domains and lipid-protein interactions in biological membranes. *Chem. Phys. Lipids* **73**:139–158

Tomishige, M., Kusumi, A. 1999. Compartmentalization of the erythrocyte membrane by the membrane skeleton: Intercompartmental hop diffusion of Band 3. *Mol. Biol. Cell* **10**:2475–2479

Tsuchida, K., Hatta, I. 1988. ESR studies on the ripple phase in multilamellar phospholipid bilayers. *Biochim. Biophys. Acta* **945**:73–80

Van, S.P., Birrell, G.B., Griffith, O.H. 1974. Rapid anisotropic motion of spin labels: Models for motion averaging of the ESR parameters. *J. Magn. Reson.* **15**:444–459

Vishnyakova, E.A., Ruuge, A.E., Golovina, E.A., Hoekstra, F.A., Tikhonov, A.N. 2000. Spin-labeling study of membranes in wheat embryo axes; 1. Partitioning of doxyl stearates into the lipid domains. *Biochim. Biophys. Acta* **1467**:380–394

Vist, M.R., Davis, J.H. 1990. Phase equilibria of cholesterol/dipalmitoylphosphatidylcholine mixtures: ^{2}H nuclear magnetic resonance and differential scanning calorimetry. *Biochemistry* **29**:451–464

Welti, R., Glaser, M. 1994. Lipid domains in model and biological membranes. *Chem. Phys. Lipids* **73**:121–137

Žuvič-Butorac, M., Müller, P., Pomorski, T., Libera, J., Herrmann, A., Schara, M. 1999. Lipid domains in the exoplasmic and cytoplasmic leaflet of the erythrocyte membrane: a spin label approach. *Eur. Biophys. J.* **28**:302–311

Žuvič-Butorac, M., Križ, J., Simonič, A., Schara, M. 2001. Fluidity of the myelin sheath in the peripheral nerves of diabetic rats. *Biochim. Biophys. Acta* **1537**:110–116